

Project Report on

# **Modelling and Simulation of Micro-channel Reactor Using FLUENT Software**

In partial fulfilment of the requirements of  
Bachelor of Technology (Chemical Engineering)

Submitted By  
**Avinash Moharana (Roll No.10600010)**  
Session: 2009-10

Under the guidance of **Prof. B. Munshi**



**Department of Chemical Engineering**  
**National Institute of Technology**  
**Rourkela-769008**  
**Orissa**



## National Institute of Technology Rourkela

### CERTIFICATE

This is to certify that that the work in this thesis report entitled —”Modelling and Simulation of micro-channel reactor using fluent software” submitted by Avinash Moharana in partial fulfilment of the requirements for the degree of Bachelor of Technology in Chemical Engineering Session 2006-2010 in the department of Chemical Engineering, National Institute of Technology Rourkela, is an authentic work carried out by him under my supervision and guidance.

To the best of my knowledge the matter embodied in the thesis has not been submitted to any other University /Institute for the award of any degree.

Date:

Prof. B. Munshi  
Department of Chemical Engineering  
National Institute of Technology  
Rourkela - 769008

## ACKNOWLEDGEMENT

With a feeling of great pleasure, I express my sincere gratitude to **Prof. Basudeb Munshi** for his superb guidance, support and constructive criticism, which led to the improvements and completion of this project work. I am also thankful to **Prof. Madhushree Kundu** for her timely support and cooperation.

I am thankful to **Mr. H.M. Jena** for acting as project coordinator.

I am also grateful to **Prof. S.K. Agarwal**, Head of the Department, Chemical Engineering for providing the necessary opportunities for the completion of this project.

Avinash Moharana (Roll: 10600010)

4th year

B. Tech.

Department of Chemical Engineering

National Institute of Technology, Rourkela

## ABSTRACT

Presented here is an insight of the momentum and energy transport phenomena occurring in a micro-channel with non-continuum (slip flow) boundary conditions. The following context deals with, 'FLUENT simulation of flow and energy based calculations using pressure correction-based iterative SIMPLE algorithm with 1<sup>st</sup> order upwind scheme in convective terms to simulate a steady incompressible two-dimensional flow through a micro-channel'. In the present work, the slip flow of liquid through a micro-channel has been modelled using a slip length assumption instead of using conventional Maxwell's slip flow model, which essentially utilizes the molecular mean free path concept and is extended to determine the temperature variation in the channel. The models developed, following this approach, forms a basis to the physics of liquid flow and energy transport through micro-channels.

## Table of Contents

<b>NOMENCLATURE</b> .....	vi
<b>LIST OF FIGURES</b> .....	vii
<b>1.INTRODUCTION</b> .....	1
1.1 General .....	2
1.2 A brief introduction to FLUENT .....	3
<b>2. TRANSPORT PROCESSES IN MICRO CHANNEL REACTOR</b> .....	6
2.1 Modelling of the governing equations .....	7
<b>3. FLUENT SIMULATION</b> .....	14
3.1 Defining the Problem .....	15
3.2 Approach to the simulation .....	16
3.3 Velocity Profile .....	16
3.4 Interpretation .....	17
3.5 Temperature Profile .....	19
<b>4. RESULTS &amp; DISCUSSION</b> .....	20
4. 1 Flow profile .....	21
4. 2 Temperature profile .....	23
4. 3 Comparison of theoretical values with that obtained from fluent .....	25
<b>5. CONCLUSION</b> .....	28

## References

**Nomenclature:**

$x$ : Axial distance;

$v_x, u$ : Axial velocity;

$u_w$ : Axial velocity at the wall (slip velocity);

$b$ : Channel clearance (width);

$L$ : Channel length;

$\rho$ : Density of the working fluid;

$\varphi_v$ : Dissipation function;

$T_\infty$ : Free stream temperature;

$u_\infty$ : free stream velocity;

$\delta$ : Momentum boundary layer thickness;

$\vartheta$ : Momentum diffusivity;

$y$ : radial distance (from the wall);

$v_y, v$ : radial velocity;

$p$ : ratio of thermal to momentum boundary layer thickness;

$Re$ : Reynolds number;

$\tau$ : Shear stress;

$L_s$ : slip length;

$c_p$ : specific heat capacity of the working fluid;

$P$ : static pressure in the channel ( $x$ );

$\delta_t$ : Thermal boundary layer thickness;

$k$ : Thermal conductivity;

$\mu$ : viscosity of the working fluid;

$T_w$ : wall temperature;

## List of Figures

Fig. 2.1: Slip length for slip flow condition on solid surface .....	7
Fig.3.1.1: Micro-channel for 1D flow.....	15
Fig.3.3.1: Variation of x-shear stress with axial distance(x) .....	17
Fig 3.4.1: Extended micro-channel .....	18
Fig.3.4.2a: x-shear stress vs axial distance for extended micro-channel.....	19
Fig 3.4.2b: y-shear stress vs x for extended micro-channel .....	19
Fig 4.1.1: Radial velocity through the channel .....	21
Fig 4.1.2: Axial velocity (u) at different values of x for Re=10 .....	21
Fig 4.1.3: Slip velocity along the micro-channel length.....	22
Fig 4.1.4: Axial velocity along the centreline of the channel for different Re .....	22
Fig 4.1.5: The longitudinal pressure distribution at the channel centreline for different Re ...	23
Fig 4.2.1: Static Temperature variation with axial distance for different Re .....	24
Fig 4.2.2: Static temperature vs axial distance at different y.....	24
Fig 4.2.3: Static Temperature variation w.r.t y at different x .....	25
Fig 4.3.1a: Comparison of theoretical temp. with simulated result at y=0.5 mm from the wall .....	25
Fig 4.3.1b: Comparison of theoretical temp. with simulated result at y=0.25 mm from the wall .....	26
Fig 4.3.2a: Comparison of theoretical temp. with simulated result at x=1 mm from the entrance .....	26
Fig 4.3.2b: Comparison of theoretical temp. with simulated result at x=5mm from the entrance .....	27
Fig 4.3.2c: Comparison of theoretical temp. with simulated result at x=2 cm from the entrance .....	27

# CHAPTER -1

## INTRODUCTION

## 1.1 INTRODUCTION TO MICRO-FLUIDICS

With the growing progress in the field of miniaturization a new field known as microelectro-mechanical systems (MEMS) came into picture. The fabrication of MEMS devices called for a new discipline employing fluid flows operating under unusual and unexplored conditions namely micro-fluidics. Micro-fluidics is an area of science and engineering in which fluid behaviour differs from conventional flow theory primarily due to non-continuum effects, surface dominated effects, and low Reynolds number effects induced by the small length scale of the micro-flow systems.

The classification proposed by Mehendale *et al* <sup>[1]</sup> and Kandlikar and Grande<sup>[2]</sup> categorized the range from 1 to 100  $\mu\text{m}$  as micro-channels. In micro-fluidics, theoretical knowledge for gas flows is currently more advanced than that for liquid flows. Concerning the gas flow through micro-channels, the issues are actually more clearly identified; the main micro-effect that results from shrinking down of device size is 'rarefaction'. In the continuum fluid transport theory, governed by the Navier–Stokes equations, it is assumed that the state variables do not vary appreciably over the length and time scales compared with the molecular mean free path and molecular relaxation time. The local density oscillation near the solid–liquid interface of the micro-channels, significant deviation of liquid viscosity compared with the bulk value, may not necessarily mean the breakdown of continuum theory; at the same time, it is important to understand how the continuum theory works in a micro-flow. There were no evidences that continuum assumptions were violated for the micro-channels tested, most of which had hydraulic diameters of 50  $\mu\text{m}$  or more. There is a clear need for additional systematic studies that carefully consider each parameter influencing transport in micro-channels.

Before going into detail on the transport processes it would be wise to discuss the differences in a micro to macro reactor w.r.t. the optimum process efficiency. Micro-channel reactors are increasingly used in many fields of industry due to the capabilities exceeding those of traditional macro-scale reactors. The high heat and mass transfer rates in micro-channel reactors allow the reaction to be performed under more aggressive conditions with higher yields (Jensen, 2001). The surface to volume ratio can be higher up to 10,000-50,000  $\text{m}^2 \text{m}^{-3}$  (Minsker and Renken, 2005) providing drastically higher heat and mass transfer rates than the traditional chemical reactors. Thus, micro-reactors can remove heat much more efficiently than traditional chemical reactors and can perform safely for highly exothermic or

endothermic reaction. Therefore, high reaction temperature is possible with micro-channel reactors and leads to reduced reactor volumes. Moreover, less amount of catalyst used improves the energy efficiency and reduces the operational costs.

Another benefit of micro-channel reactors is that if the system fails the amount of accidentally released chemicals is rather small and it could be easily controlled. The integrated sensor and control units could allow the failed reactor to be isolated and replaced while other parallel units continued production (Jensen, 2001). Besides the benefits of the micro-channel reactors, some problems still remain in the system. Clogging is one of the main problems occurring in the particle containing processes, for example, catalytic reactions. Clogging has been identified as the biggest problem, however, the particle containing processes also cause rather high pressure drop through the flow channel. These two main factors have to be considered while operating with micro-channel reactor.

The following study is an attempt on describing incompressible flow through micro-channels by analytical method and hence comparing the results with that obtained from a commercial software package for simulation (FLUENT). For liquids and gases the fluid particle need not be as large as  $10\ \mu\text{m}$ , but rather be on the order of  $10\ \text{nm}$  and a few hundreds of nanometers, respectively, to be considered as macroscopic. Therefore for ordinary liquids (fluids), the current micro fluidic devices are subjected to the rules of classical fluid mechanics.

## **1.2 A brief introduction to FLUENT**

Fluent is a general-purpose CFD code based on the finite volume method based on a collocated grid. FLUENT technology offers a wide variety of physical models that can be applied to a wide array of industries. Some of its features include the following:

- **Dynamic and Moving Mesh:** The user simply sets up the initial mesh and prescribes the motion, while FLUENT software automatically changes the mesh to follow the motion prescribed. This is useful for modelling flow conditions in and around moving objects.
- **Heat Transfer, Phase Change, and Radiation:** FLUENT software contains many options for modelling convection, conduction and radiation.
- **Multiphase:** It is possible to model several different fluids in a single domain with FLUENT.
- **Turbulence:** A large number of turbulence models are used to approximate the effects of turbulence in a wide array of flow regimes.

- Acoustics: The acoustics model lets users perform "on-the-fly" sound calculations.
- Reacting Flows: FLUENT technology has the ability to model combustion as well as finite rate chemistry and accurate modeling of surface chemistry.
- Post-processing: Users can post-process their data in FLUENT software, creating - among other things - contours, pathlines, and vectors to display the data.

Before simulating the problem we first need to model the problem with software named GAMBIT. Speaking of GAMBIT, it can be well said as a geometric modelling and grid generation tool i.e. often shipped with FLUENT technology. It allows the users to create their own geometry or import geometry from most CAD packages. It can automatically mesh surfaces and volumes while allowing the user to control the mesh through the use of sizing functions and boundary layer meshing.



## CHAPTER -2

# TRANSPORT PROCESSES IN MICRO CHANNEL REACTOR

Apart from wetting, adsorption, and electro kinetic effects, the slip phenomena play an important role in modelling liquid flow through micro-channel. Helmloltz and Von Piotrowski found evidence of slip between a solid surface and a liquid and later Brodman verified their results. Navier (1823) was the first to model partial slip at the wall for liquids well before Maxwell's slip model for gases (1879). Analytic slip-flow studies have traditionally been based on the continuum form of Navier-Stokes equations and energy equation with the slip-flow effects concentrated in the additional terms in the tangential velocity and temperature boundary conditions <sup>[3]</sup>. These new boundary conditions represent velocity slip and temperature jump conditions at the gas-surface interface. Slip flow condition is well described by introducing the concept of slip length. Slip length is the distance behind the solid-liquid interface at which the velocity extrapolates to zero. Liquid flow in a micro-channel becomes fully developed after a short entrance length so that it can be modelled as a two-dimensional flow. In view of this, present study aims for two-dimensional micro-channel flow simulation with non-continuum (slip velocity) boundary conditions.

The slip velocity at the wall as given by Navier is

$$v_x]_{\text{wall}} = L_s \left( \frac{\partial v_x}{\partial n} \right)_{\text{wall}}$$

Where  $L_s$  is the slip length;  $n$  is the normal coordinate pointing inward from the channel wall. The above proposition is valid both for gas and liquid flow.

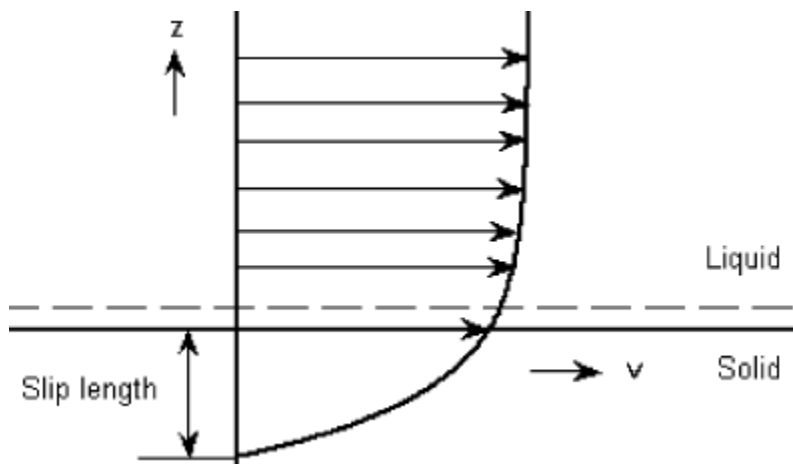


Fig. 2.1: Slip length for slip flow condition on solid surface

## 2.1 Modelling of the governing equations for one dimensional incompressible flow through a heated surface micro-channel with a two-dimensional velocity and Temperature field:

Assumptions:

- (1) The fluid is Newtonian in nature with constant viscosity and is incompressible.
- (2) The flow is laminar and the shear rates involved are small.
- (3) Gravity effects are neglected.
- (4) We also assume that  $u = u(x, y)$ ;  $v = w = 0$  and  $T = T(x, y)$ .

Let us consider no slip flow condition and model the governing equations very close to the wall surface.

- By boundary layer theory the flow near a solid surface with no slip condition is given by:

$$u = u_{\infty} \left[ \frac{3y}{2\delta} - \frac{1y^3}{2\delta^3} \right]$$

where,  $u$ : velocity in  $x$ -direction (function of both  $x$  &  $y$ )

$\delta = \delta(x)$ : boundary layer thickness

The above equation is derived considering the profile to be a polynomial function of the distance from the wall ( $y$ ) satisfying the specified boundary conditions.

Let the best suited curve be given by

$$u = c_1 + c_2 y + c_3 y^2 + c_4 y^3 \quad (2.1.1)$$

The boundary conditions are:

B1: At  $y=0$ ;  $u=0$  : No slip condition;

B2: At  $y=b/2$ ;  $u=u_{\max} = u_{\infty}$  : Bulk velocity;

B3: At  $y=0$ ;  $\frac{d^2u}{dy^2} = 0$  : Constant shear at the wall (at a particular  $x$ );

B4: At  $y=\delta$ ;  $\frac{du}{dy} = 0$  : Shear at  $\delta$ ;

Substituting B1 in (2.1.1);  $c_1=0$

Using B3;  $c_3=0$

Using B2;  $c_2 (b/2) + c_4 (b/2)^3 = u_{\max} = u_{\infty}$

Using B4;  $c_2 + 3c_4 \delta^2 = 0$

Solving for  $c_2$  and  $c_4$ ; we get,

$$c_4 = -u_{\max} / 2 \delta^3 \text{ and } c_2 = 3u_{\max} / 2 \delta$$

Substituting in equation (2.1.1); we get,

$$u = u_{\infty} \left[ \frac{3y}{2\delta} - \frac{1}{2} \frac{y^3}{\delta^3} \right]$$

Now considering slip flow condition, the slip velocity, on the channel walls is based on the following assumptions:

(1) At a distance of  $L_s$  from the present channel wall, on both the sides, there exists an imaginary boundary wall (IBW) – rigid and solid.

(2) At the position where presently there exists a wall, it is assumed that no solid wall is present and there exists a velocity for the fluid moving over the IBW.

The velocity is equal to the slip velocity in the present case.

Considering the above steps, and solving for the wall velocity by replacing  $y$  with  $L_s$  would yield us the slip velocity as,

$$u_w = u_{\infty} \left[ \frac{3}{2} \left( \frac{L_s}{\delta} \right) - \frac{1}{2} \left( \frac{L_s}{\delta} \right)^3 \right] \quad (2.1.2)$$

The problem now is to find the free-stream velocity,  $u_{\infty}$ , and the boundary layer thickness,  $\delta$ . As we are dealing with micro-channels, it can be expected that the velocity of the fluid on the IBW shall be small enough to consider the flow as laminar. This consideration will yield the expression for the boundary layer thickness,  $\delta$ , as:

$$\delta = \sqrt{\frac{280 \vartheta x}{13 u_{\infty}}}$$

Where  $\vartheta$ : momentum diffusivity

The free-stream velocity ( $u_{\infty}$ ) is nothing but the incident velocity. Thus, combining the above expressions, we get an expression for the slip velocity as a function of  $\delta$ , that is, a function of

$x$ . mathematically, it can be derived that the slip velocity is actually an inverse function of axial dimension. The radial velocity component is assumed to be zero on the channel walls.

At the entrance of the channel, the radial velocity component is set to zero, and a uniform velocity  $u_\infty$  for the axial velocity component is assumed.

Because of the elliptic nature of the flow fields investigated, the outlet boundary condition will have some influence on the development of the upstream flow. The normal gradient of all dependent variables at the outlet are constants. This is equivalent to the requirement of the second derivative of any dependent variable becoming zero. Using this condition, the numerical procedure is stable and convergent for those flows, which eventually reaches a steady state condition at the outlet.

$$\frac{\partial^2 u}{\partial x^2} = \frac{\partial^2 v}{\partial x^2} = 0$$

Therefore the velocity profile in the micro-channel incorporating the slip condition can be deduced as follows. The boundary conditions to the derivation can be modified to:

$$B1': \text{ At } y=0; u= u_{wall};$$

$$B2': \text{ At } y=b/2; u= u_{max} \neq u_\infty$$

Here  $u_{max}$  is function of axial distance( $x$ ) from the entrance. Substituting these along with B3 and B4 in equation (2.1.1) the velocity profile comes out to be

$$\frac{u-u_{wall}}{u_{max}-u_{wall}} = \frac{3y}{2\delta} - \frac{1y^2}{2\delta^2} \quad (2.1.3)$$

Similarly the temperature profile in the micro channel can be reasoned to be of the form

$$\frac{T-T_{wall}}{T_\infty-T_{wall}} = \frac{3y}{2\delta_t} - \frac{1y^2}{2\delta_t^2} \quad (2.1.4)$$

Where,  $T_{wall}$ : wall temperature;

$T_\infty$ : bulk temperature (temperature of the entering fluid)

$\delta_t$ : thermal boundary layer thickness

The thermal boundary layer thickness is again a function of momentum boundary layer which is determined by considering energy balance around a control volume element in the flow boundary.

- Apart from the empirical approach, the velocity profile can also be determined by solving the continuity and the momentum balance equation. The postulates for the flow phenomena are

$v_x = u(x, y)$ ;  $v_y \approx 0$  : negligible radial velocity ;  $P = P(x)$  : Pressure only function of  $x$

with boundary conditions :

B1: At  $y = -L_s$ ;  $u = 0$  : slip length( $L_s$ ) distance away from wall

B2: At  $y = \delta$  ;  $\frac{du}{dy} = 0$  : shear at  $\delta$

Hence, continuity equation:

$$\frac{\partial v_x}{\partial x} + \frac{\partial v_y}{\partial y} = 0$$

and momentum equation:

$$\rho \left( v_x \frac{\partial v_x}{\partial x} + v_y \frac{\partial v_y}{\partial y} \right) = - \frac{dP}{dx} + \mu \left[ \frac{\partial^2 v_x}{\partial x^2} + \frac{\partial^2 v_x}{\partial y^2} \right]$$

equation reduces to (assuming  $v_y$  negligible)

$$- \frac{dP}{dx} + \mu \left[ \frac{\partial^2 v_x}{\partial y^2} \right] = 0$$

Solving for  $v_x$  using B1 and B2 we get,

$$v_x = u = \frac{1}{\mu} \left( \frac{dP}{dx} \right) \left[ \frac{y^2}{2} - \delta(y + L_s) - \frac{L_s^2}{2} \right] \quad (2.1.5)$$

For flow in a micro channel both the equations (2.1.3) and (2.1.5) equally describe the flow very near to the wall but at  $y \rightarrow b/2$ , radial velocity component is induced and hence flattening of the velocity profile occurs. This results in the decreasing magnitude of the axial velocity component after a peak maxima at about  $x_0$  (where  $b/2 = \delta$ ).

- Expression for thermal boundary layer thickness ( $\delta_t$ ):

Unlike the case in classical macro-channel flow, here the concept of Prandtl no. as the ratio of momentum to thermal boundary layer thickness is quite not true. This is because the flow completely lies in the boundary layer region and hence the actual thermal boundary layer thickness is unknown. The following is an attempt on to derive an expression for the same.

For flow over a heated boundary surface the following assumptions are made:

$$T=T(x,y); \frac{\partial^2 T}{\partial x^2} = 0 : \text{considering linear variation with } x$$

Hence the energy balance equation reduces to

$$\rho c_p v_x \frac{\partial T}{\partial x} = k \frac{\partial^2 T}{\partial y^2} + \mu \varphi_v \quad (2.1.6)$$

where  $\varphi_v$ : Dissipation function =  $\left(\frac{\partial v_x}{\partial y}\right)^2$

$$\Rightarrow v_x \frac{\partial T}{\partial x} = \alpha \frac{\partial^2 T}{\partial y^2} + \frac{1}{Pr} \left(\frac{\partial v_x}{\partial y}\right)^2$$

Let the velocity profile be given by equation (2.1.3) and temperature by equation (2.1.5), hence by substituting and integrating w.r.t.  $y$ , we get

$$\frac{d}{dx} \int_0^y (u T) dy = \alpha \frac{dT}{dy} \Big|_0^y + \frac{1}{Pr} \frac{9}{4} \left(\frac{u_{co}-u_{wall}}{\delta}\right)^2 \int_0^y \left(1 - \left(\frac{y}{\delta}\right)^2\right)^2 dy$$

$$\text{For } y=\delta_t; \frac{dT}{dy} = 0$$

$$\text{And } y=0; -k \frac{dT}{dy} = \text{wall flux}$$

This is the integral equation of the boundary layer for constant properties and constant free stream temperature  $T_\infty$ . Since laminar flow is considered, the viscous dissipation term is very negligible and hence is neglected unless the velocity in the flow field becomes very large.

$$\frac{d}{dx} \int_0^{\delta_t} (u T) dy = \alpha \frac{dT}{dy}$$

$$\int_0^{\delta_t} (u T) dy = \beta \theta \left(\frac{3}{4} p^2 \delta - \frac{3}{20} p^2 \delta - \frac{3}{20} p^4 \delta + \frac{1}{28} p^4 \delta\right) + \theta u_w \left(\frac{3}{4} p - \frac{1}{8} p\right) + \beta T_w \left(\frac{3}{4} p^2 \delta - \frac{1}{8} p^4 \delta\right)$$

Where,  $p = \delta_t / \delta$ ;  $\theta = (T_\infty - T_w)$ ;  $\beta = (u_\infty - u_w)$

Neglecting higher order terms of  $p$ ,

$$\int_0^{\delta_t} (u T) dy = \theta u_w \frac{5}{8} p$$

$$\Rightarrow \frac{d}{dx} (\theta u_w \frac{5}{8} p) = \alpha \theta \frac{3}{2 \delta_t}$$

$$\Rightarrow \frac{d}{dx} p = \frac{5\alpha}{8 u_w} \left( \frac{1}{p \delta} \right)$$

Hydrodynamic boundary layer thickness ( $\delta$ ) is obtained by substituting the velocity profile into the von Karman integral balance [5] to get

$$\delta = \sqrt{\frac{280 \vartheta x}{13 v_\infty}}$$

Hence we get,

$$\frac{p^2}{2} = \frac{12 \alpha \sqrt{v_\infty / \vartheta}}{5 u_w} 2 \sqrt{x} + C$$

At  $x=0$ ;  $p=0 \Rightarrow C=0$

$$\Rightarrow \delta_t = 4 \sqrt{\frac{3\alpha}{u_w} \left( \frac{\vartheta}{u_\infty} \right)^{0.5} x^{0.75}} \quad (2.1.7)$$

Similarly by considering the velocity profile as in equation (2.1.5), the thermal boundary layer thickness is found to be:

$$\delta_t = \frac{3}{2} \frac{\alpha \mu}{(dP/dx) T_\infty} \left( \frac{2\delta}{L_s + 2\delta} \right) \quad (2.1.8)$$

Therefore substituting either of these equations in equation (2.1.4) we get the required temperature profile for slip flow over a heated boundary surface.

The analytic equation obtained, forms the base for solving the flow equations. In order to predict the phenomena, the steady state equations are solved by using the commercial software package FLUENT 6.3.26 which uses a numerical iterative method for the simulation.



# CHAPTER -3

## FLUENT SIMULATION

### 3.1 Defining the Problem

In the current simulation we aim at studying the flow phenomena and the temperature distribution occurring in a micro-channel. With reference to the simulations done in <sup>[4]</sup>, we choose the same channel dimensions so as to have a discussion on the results obtained.

The channel considered is viewed as two parallel plates placed one over the other extending into the  $z$ -direction, and the flow is in the  $x$ -direction. It has been assumed that the  $z$ -directional dimension is equal to unity. The channel clearance length ( $b$ ) is 1mm. As far as the bulk properties of the fluids are concerned, 1mm is still a scale governed by the classical laws of simple liquids and ideal gases under normal pressure. Therefore, for ordinary liquids (fluids), the current micro fluidic device is subjected to the rules of classical fluid mechanics. The channel length ( $L$ ) considered is equal to 10cm. Again in reference to <sup>[4]</sup> the inlet Reynolds number is taken as 10.

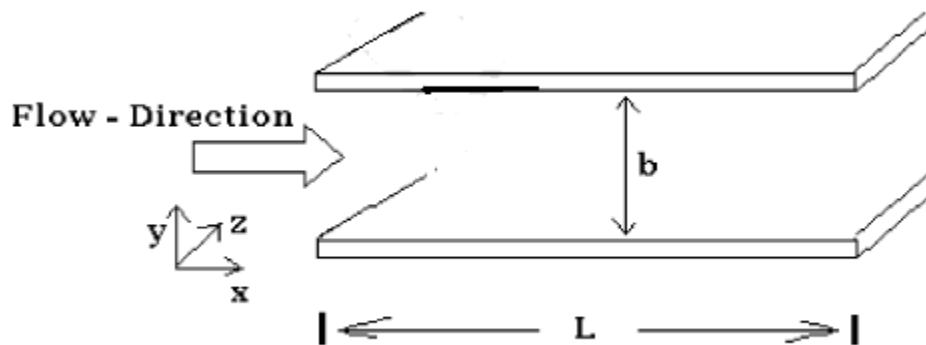


Fig. 3.1.1: Micro-channel for 1D flow

### 3.2 Approach to the simulation

The above 2D problem geometry is created (to the given dimensions) by using GAMBIT 2.2.30 software. Then the geometry is meshed (100\*100, let) into smaller cells. Higher the no. of cells the greater is the accuracy with more rigorous calculations and lower convergence limit.

This then is exported as a 2D mesh file to be solved in FLUENT 6.3.26.

Now specifying the boundary conditions and choosing a suitable solver we initialize the problem and then run the iteration for the solution.

### 3.3 Velocity Profile

As discussed above the mesh file is imported into FLUENT 6.3.26 and the boundary values are specified. The working fluid considered is liquid water with outlet pressure of 1 atm.

In specifying the boundary conditions,

- The inlet velocity corresponding to a Reynolds no. of 10 is calculated as 0.01 m/s.
- At the wall the slip velocity is accounted by specifying the shear stress in x direction.

The solver specified uses a pressure correction based iterative SIMPLE algorithm with the discretization done with 1<sup>st</sup> order upwind scheme.

Theoretically the shear stress at the wall is calculated by the following expression:

$$\tau_{ij} = -\mu \left( \frac{\partial v_j}{\partial x_i} + \frac{\partial v_i}{\partial x_j} \right)$$

Since the wall velocity is a function of the position x, so as a first approximation the shear value specified is a constant averaged over the total length of the channel.

$$\tau_x = \tau_{xx} + \tau_{yx} = 0.001 \text{ Pa}$$

Alternately, the function generated for shear stress in terms of the position variable, x, can directly be coupled by defining a user defined function (udf). The udf coded is as follows:

```
#include "udf.h"

DEFINE_PROFILE(wall_shear_x, thread, i)
{
    double x[ND_ND];
    face_t f;
    double y;
```

```

begin_f_loop(f,thread)
y=x[1];

F_PROFILE(f,thread,i)= -0.0000000001* (0.15* sqrt(10000*
(y+0.0000001))-0.006/sqrt(10000*(y+0.0000001)))-0.00001*(0.0237*
sqrt(10000*(y+0.0000001))-0.00000003795/sqrt(10000*(y+0.0000001)));

end_f_loop(f,thread)
}

```

The values obtained are in close resemblance to that calculated theoretically. Other methods for shear stress evaluation involve defining a line/rake at the required surface and hence obtaining the wall fluxes (in *XY plot* option). For this we modify the considered micro-channel by increasing the channel width by twice the slip length ( $L_s$ ) (i.e. the imaginary boundary layer). Doing so we solve for no slip flow condition and subsequently after simulation we evaluate the wall fluxes at  $y = L_s$ .

The wall shear stress obtained by the above methods are summarised as follows:

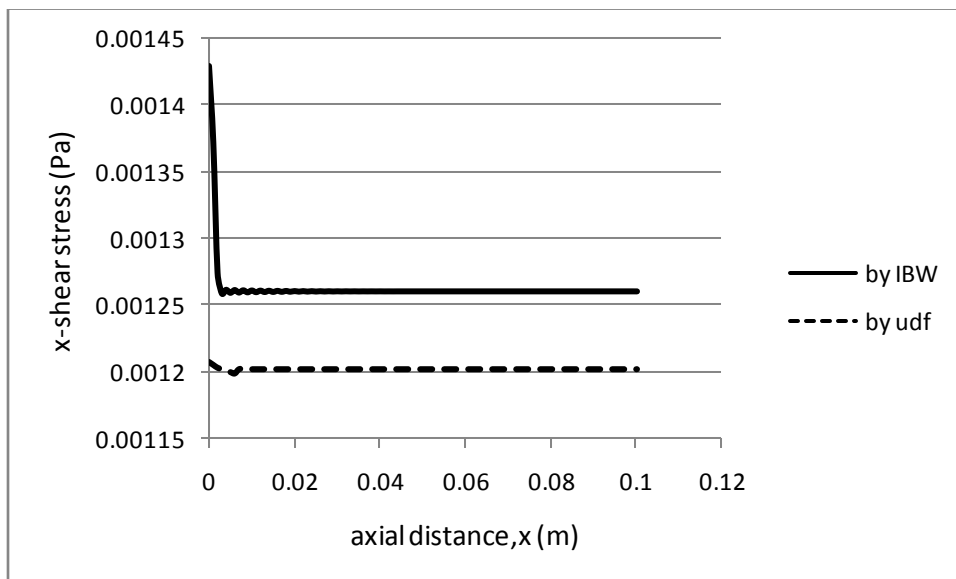


Fig. 3.3.1: Variation of x-shear stress with axial distance(x)

### 3.4 Interpretation

It is found that there exists no y-shear at the wall which is physically incorrect. This is because unlike flow through macro-channels, the velocity here is also a function of x even in

the fully developed regime. This induces a velocity gradient in  $y$  direction though practically very negligible in comparison to  $x$  directional shear.

Existence of dominant  $y$ -shear stress can be shown by introducing radial velocity component into the micro-channel, therefore consider an extended micro-channel as shown:

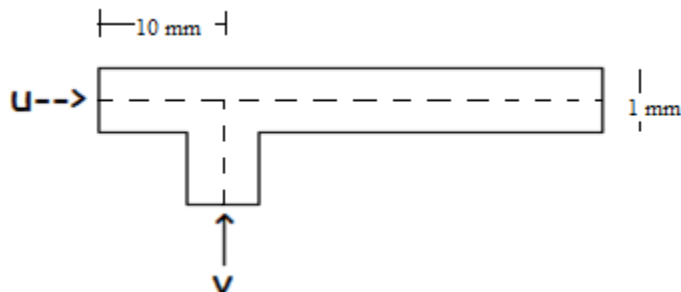


Fig 3.4.1: Extended micro-channel

On simulation with inlet velocity of 0.01 m/s, the shear stress on the surface  $y=0$ ,  $0 < x < 0.1$  m (the bottom edge) is found to be:

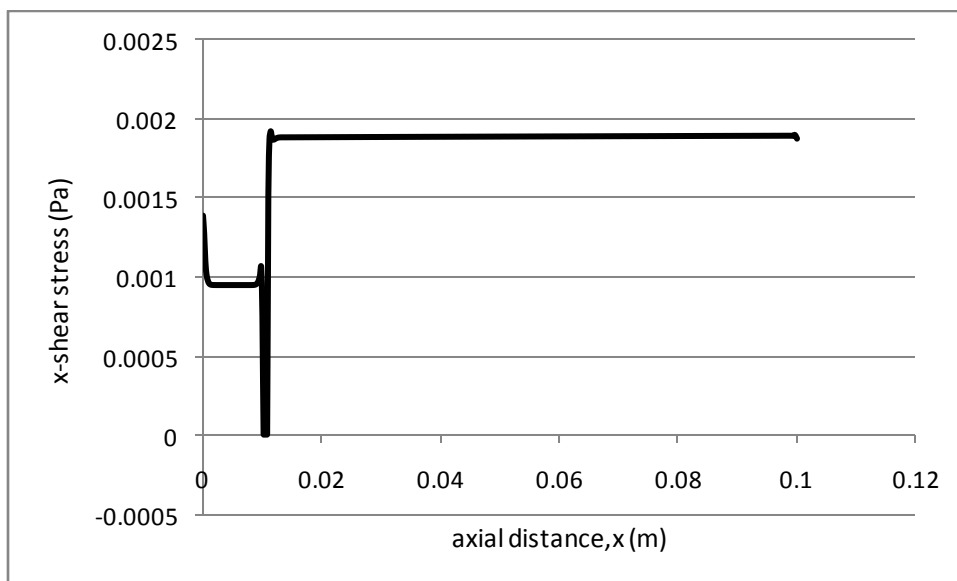


Fig. 3.4.2a:  $x$ -shear stress vs axial distance for extended micro-channel

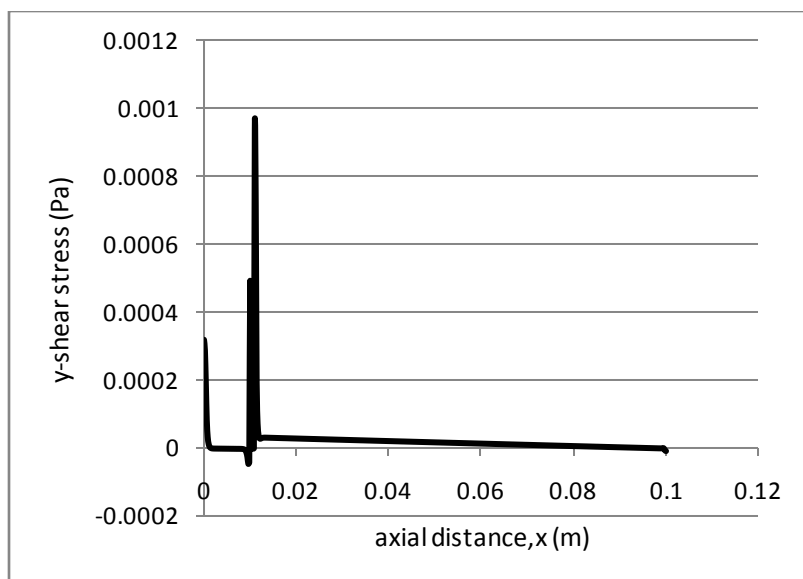


Fig 3.4.2b: y-shear stress vs x for extended micro-channel

Hence it is concluded that the computed x-shear by the software is a summation of both shear stresses acting on plane perpendicular to x axis and y-axis in the x-direction. The y-shear for 1D flow is zero.

### 3.5 Temperature Profile

For the same dimensions of the micro-channel we consider the boundary walls to be at a temperature of  $T_w$  (= 375 K). The inlet temperature of the free stream be  $T_\infty$  (= 300 K). The above parameters are fed to the software and thus in addition to flow equation, energy equation is also solved.

The simulated results are discussed in the next chapter.

# CHAPTER -4

## RESULTS AND DISCUSSION

#### 4.1 Flow profile

Figure 4.1.1 shows the radial velocity profile, along the radial direction at different  $x$  and  $Re = 10$ . At the entrance of the channel, velocity in the radial direction is very small in comparison with that in the axial direction. It is evident from Fig. 6 that after a certain value of  $x$ , at which flow has been fully developed, the change in radial velocity component is very negligible and it behaves as a one-dimensional flow.

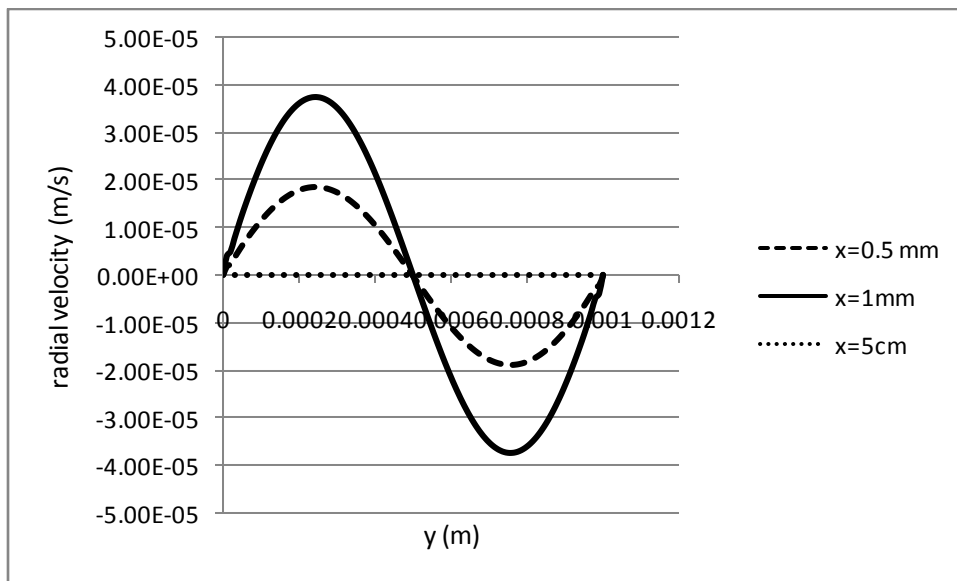


Fig 4.1.1: Radial velocity through the channel

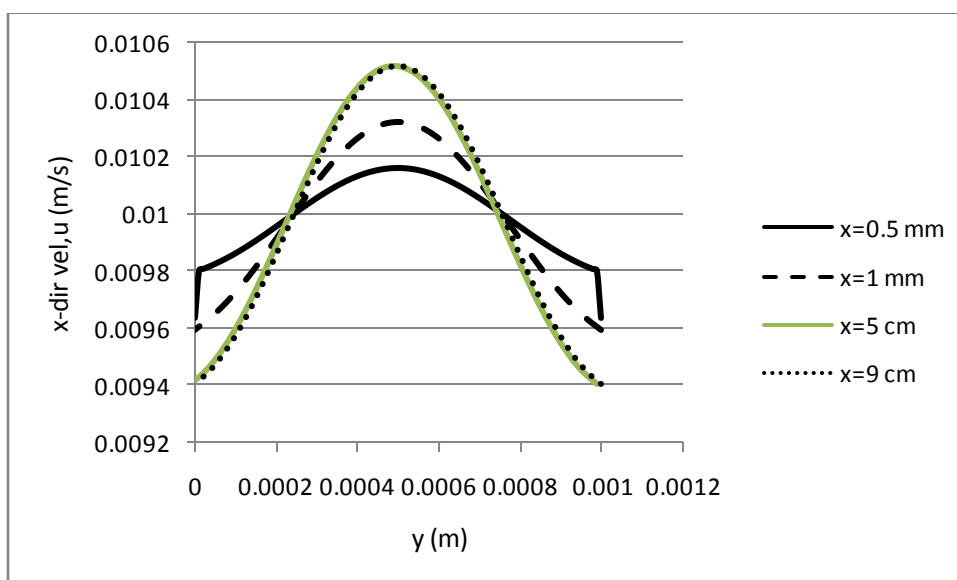


Fig 4.1.2: Axial velocity (u) at different values of  $x$  for  $Re=10$

Flattening in the velocity profile is a phenomenon that is found in one-dimensional flow problem. Figure 4.1.4 shows that along the length of the micro-channel, at the centreline and for  $Re = 10$ , the axial velocity develops to a maximum at about  $x = 1.21\text{ mm}$ , the flattening in the velocity profile begins onwards. The effect of Reynolds number on flattening in longitudinal velocity profile is shown in Fig. 4.1.4. With increasing Reynolds number the flattening effect is accelerated and at higher  $Re$  there is almost no flattening in  $u$ -profile for the complete length of the channel.

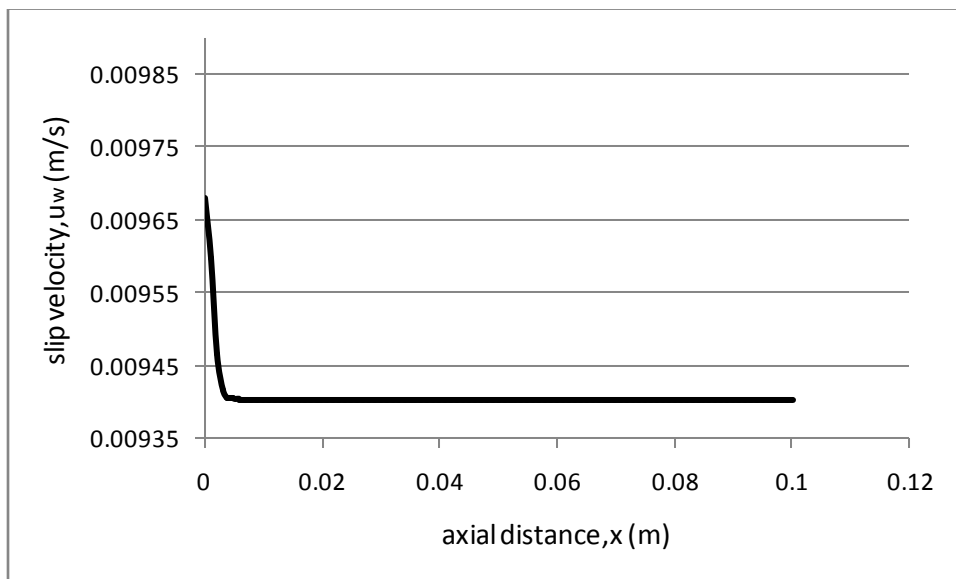


Fig 4.1.3: Slip velocity along the micro-channel length

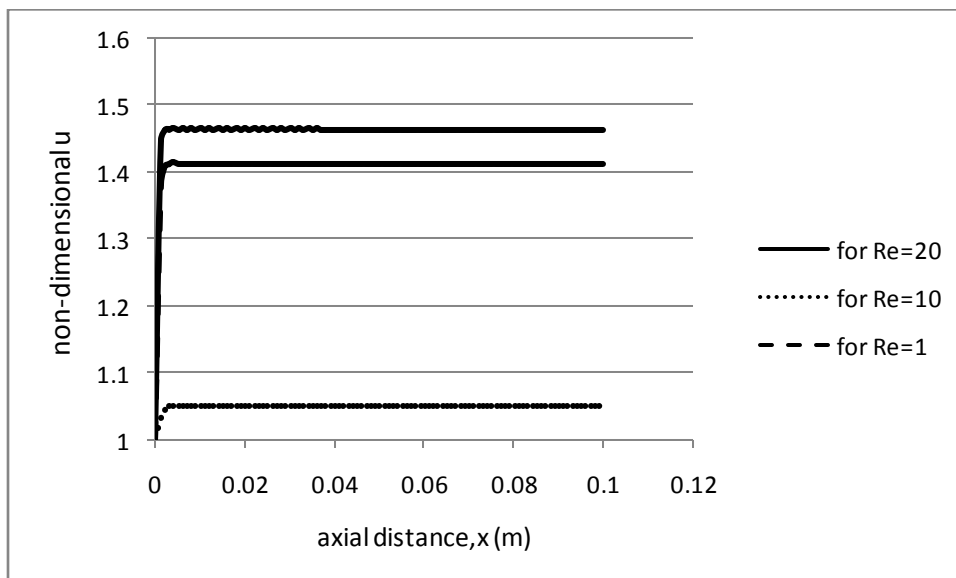


Fig 4.1.4: Axial velocity along the centreline of the channel for different  $Re$

Figure 4.1.2 shows the velocity profile in the channel with increasing axial distance. Here too the flattening effect is evident with a variable wall slip velocity at the channel boundaries.

The slip velocity is independent of the radial component of the velocity and is a decreasing function of the axial dimension as found on simulation in Fig. 4.1.3. At about  $x = 10\text{mm}$  and onwards, the slip velocity is negligible and almost constant for the remaining length. Hence the channel behaves as a mini-channel. Therefore the axial velocity ( $u$ ), beside its radial dimensional dependency, is to be considered within this short span of channel length for micro-channels in practice.

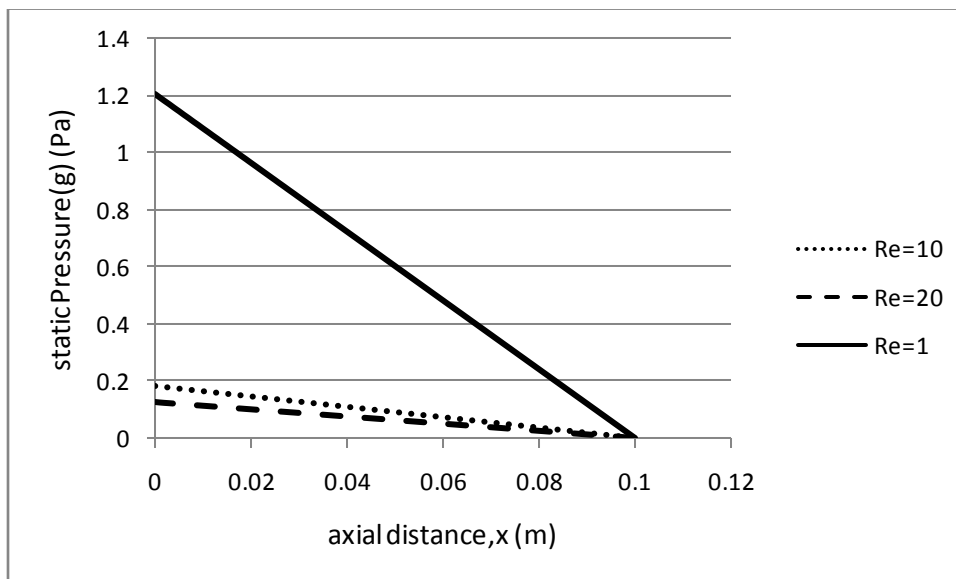


Fig. 4.1.5: The longitudinal pressure distribution at the channel centreline for different Re

Figure 4.1.5 shows the static pressure variation with increasing inlet Reynolds number. At low Reynolds number the pressure drop across the channel increases. In actual case for flow of gases, the curves tend to be non-linear which explains the compressibility effect as discussed by Chen<sup>[6]</sup>, in the numerical simulation for flow of gases through micro-channels.

## 4.2 Temperature profile

Figure 11 shows the temperature variation with changing inlet Reynolds number. As evident at higher Re the convective part is dominant and hence it requires a larger length for steady state temperature to be reached while at lower Re the diffusive heat transfer term is dominant.

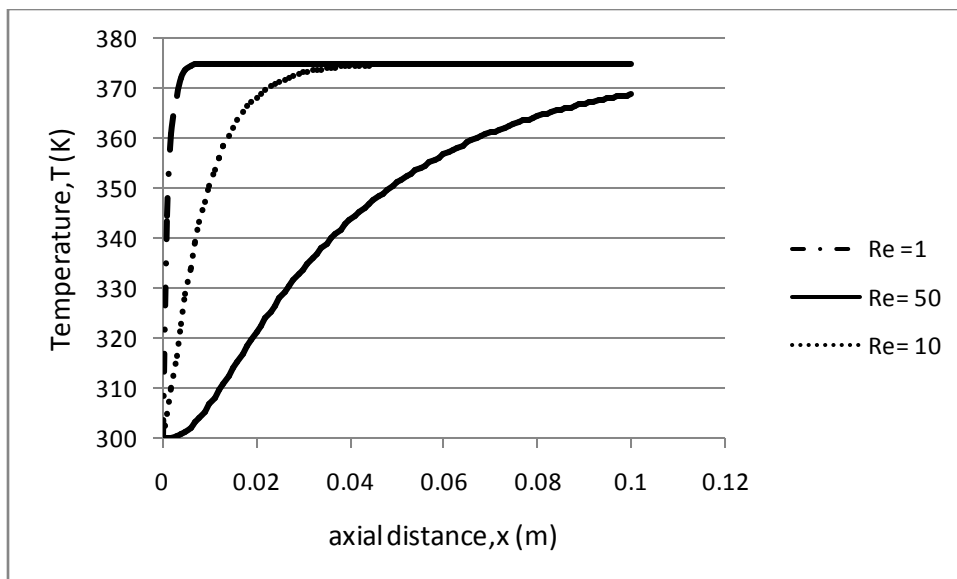


Fig 4.2.1: Static Temperature variation with axial distance for different Re

For flow through a channel of width (b) 1mm the following Temperature profiles are obtained. Figure 4.2.2 shows the variation of temperature with axial distance at different values of (y) and Figure 4.2.3 shows the temperature profile at different axial distance. For Re=10 we find the steady state profile at about  $x=35$  mm.

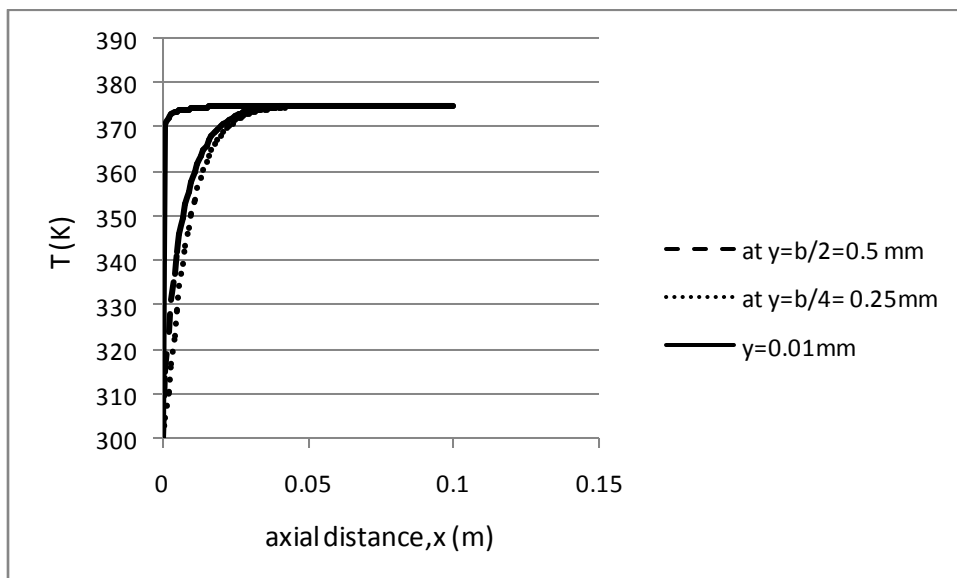


Fig 4.2.2: Static temperature vs axial distance at different y

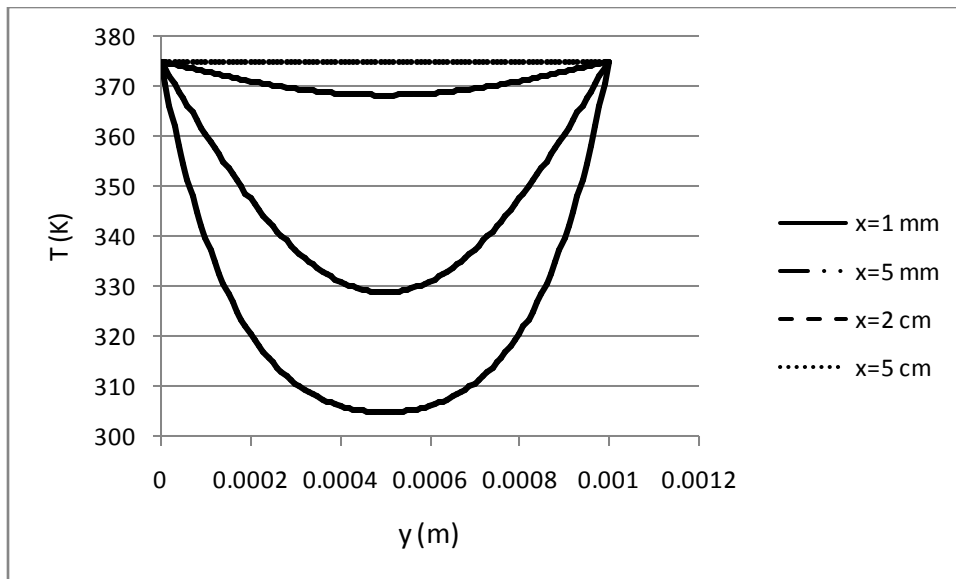


Fig 4.2.3: Static Temperature variation w.r.t y at different x

### 4.3 Comparison of theoretical values with that obtained from fluent

The modelled equations for the flow and energy transport are given by equations (2.1.1)-(2.1.8). Using these we solve for the velocity and the temperature profiles and hence compare the values with those obtained from simulation. For this we consider (case I) variation of temperature with x keeping y constant and (case II) longitudinal variation at different values of axial position.

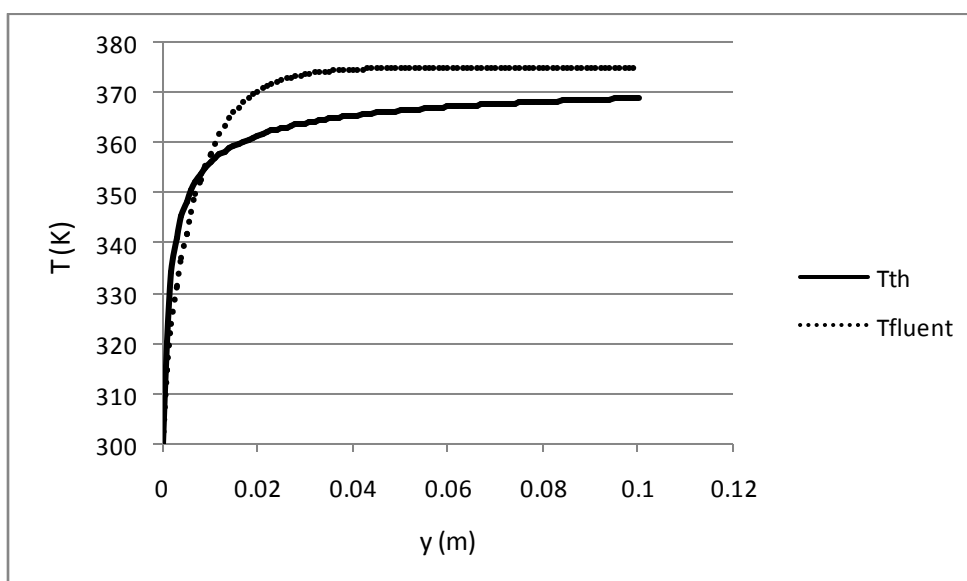


Fig 4.3.1a: Comparison of theoretical temp. with simulated result at  $y=0.5$  mm from the wall

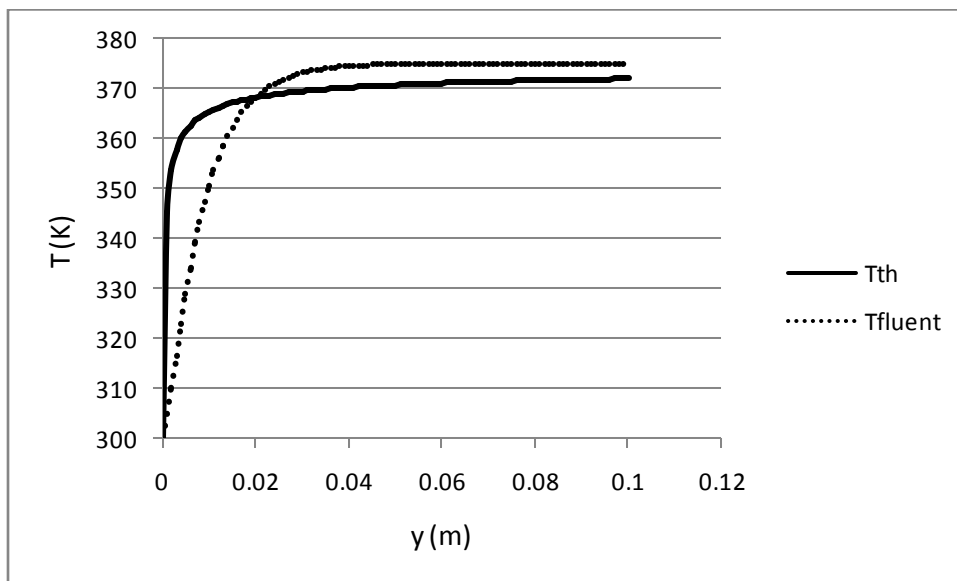


Fig 4.3.1b: Comparison of theoretical temp. with simulated result at  $y=0.25$  mm from the wall

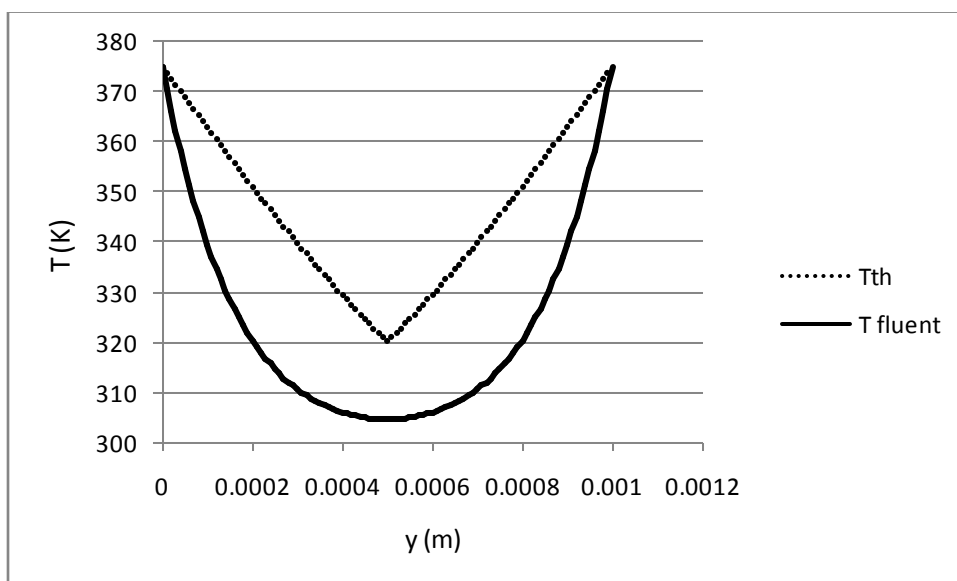


Fig 4.3.2a: Comparison of theoretical temp. with simulated result at  $x=1$  mm from the entrance

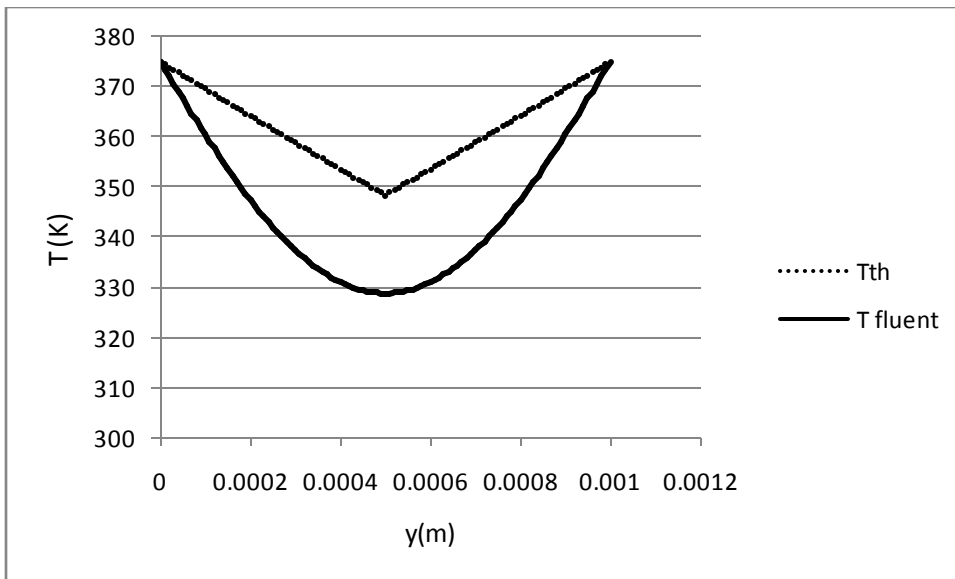


Fig 4.3.2b: Comparison of theoretical temp. with simulated result at  $x=5\text{mm}$  from the entrance

From the curves we conclude that the theoretical models developed, despite of the assumptions made, are in good match in explaining the flow and energy transport process in the channel. Therefore while solving the likes of equation (2.1.5) and (2.1.8), complexity can be eliminated by directly using an output variable from the simulation.

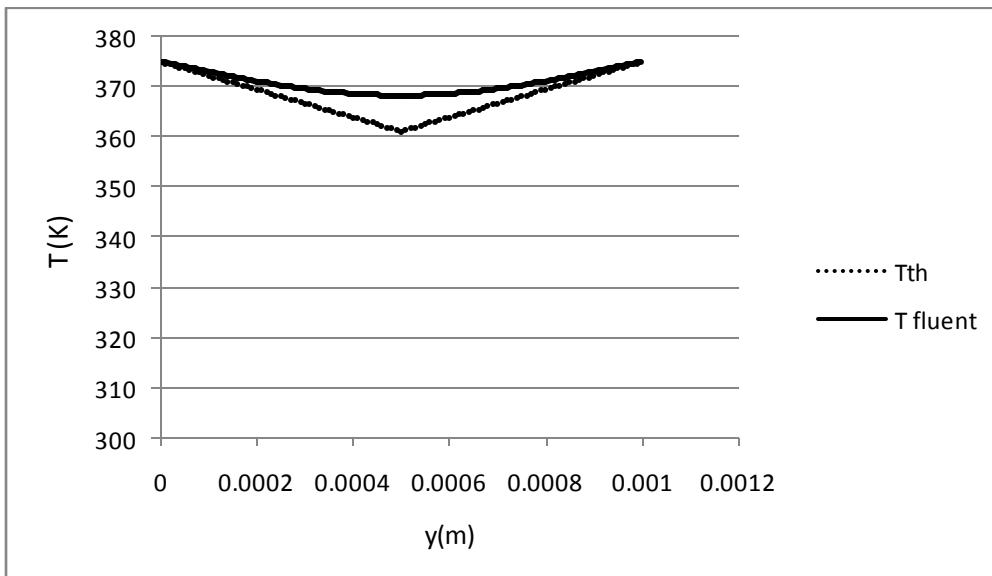


Fig 4.3.2c: Comparison of theoretical temp. with simulated result at  $x=2\text{ cm}$  from the entrance

## CHAPTER -5

## CONCLUSIONS

Keeping in view of its immense significance, this study is focused on the simulation and analysis of the micro-channel flow and energy transport. It thus gives an elementary base to the physics of the problem which would contribute in the theoretical understanding of such transport phenomena.

In micro-channel, the velocity in the radial direction is small in comparison with that in the axial direction as is evident from the simulated results. After the flow has been fully developed, the change in radial velocity component is very negligible; it behaves as a one-dimensional flow. Flattening in the velocity profile is a phenomenon that has been found on the basis of one-dimensional flow problem and on the basis of FLUENT simulation of the flow considered here. At low Reynolds number, the axial velocity maintains a slow rate of flattening and the slip velocity decreases along the axial length and finally remains constant; hence the channel after a certain length behaves as a mini-channel (i.e. a channel with micro-dimension but with negligible slip velocity).

Moreover the study of temperature variation in the channel gives an insight to the relation between inlet Peclet number with the temperature profiles obtained. This helps in times of designing and fabrication of a micro-channel reactor. The slip effect reduces the friction in micro-channel flow; hence, fluid can be driven through it with a lesser power consumption than in comparison with the flow through macro- or mini-channel. With decreasing Reynolds number the pressure drop through the channel decreases with increased contribution of the diffusive heat transfer term in the boundary layer region.

## References

- [1] S.S. Mehendale, A.M. Jacobi, R.K. Shah. *Appl. Mech. Rev.*,2003; 53, 175–193.
- [2] S.G. Kandlikar,W.J. Grande. *Heat Transfer Eng.*, 2003; 24(1),3–17.
- [3] E.G.R.,Eckert, R.M. Drake, Jr. *Analysis of Heat and Mass Transfer*, Mc-Graw-Hill, 1972, pp.467-486.
- [4] Madhusree Kundu, Krishna Vamsee and Dilip Maiti, *Research Article Simulation and analysis of flow through microchannel*, *Asia-Pac. J. Chem. Eng.* (2008).
- [5] R. Byron Bird, Warren E. Stewart, Edwin N. Lightfoot; *Transport Phenomena* (2<sup>nd</sup> ed.); pg. 135-138.
- [6] C.Chen, *J. Applied Physics*, 1956; 27(1), 1149-1152
- [7] A. Mukhopadhyay, G. Biswas, T. Sundarajan. *Int. J. Numer. Methods Fluids*, 1992; 14, 1473–1484.
- [8] B. Palm. *Microscale Thermophys. Eng.*, 2001; 5, 155–175
- [9] S. Colin. *Microfluidique*, Lavoisier – Hermès Science Publications: Paris